



Thermodynamic Analysis of a Novel Heat Pipe Based Regenerative Combined System

V. Beygzadeh^{1*}, Sh. Khalilarya², I. Mirzaee², V. Zare¹, Gh. Miri³

¹ Faculty of Mechanical Engineering, Urmia University of Technology, Urmia, Iran

² Mechanical Engineering Department, Faculty of Engineering, Urmia University, Urmia, Iran

³ Department of Business Management, National Iranian Oil Refining & Distribution Company, Tehran, Iran

ABSTRACT: A comprehensive thermodynamic analysis is presented of a new solar system for heating and power generation. Energy and exergy analyses are used to characterize the exergy destruction rate in any component and investigate solar system performance. The system composed of a solar heat pipe evaporator, an auxiliary pump, a condenser, a turbine, an electrical generator, a domestic water heater, a regenerator, a water preheater and a pump. The solar system provides heating and electricity during the summer and spring in Tabriz, Iran. The analysis involves the specification of effects of varying solar heat pipe evaporator condenser pinch point temperature, varying solar radiation intensity and varying solar heat pipe evaporator heat removal factor on the energetic and exergetic performance of the system. The performance parameters calculated are energy flow, exergy destruction rate, energetic and exergetic efficiencies. The results also showed that the main source of the exergy destruction rate is the solar heat pipe evaporator. In the solar heat pipe evaporator, 291.1 kW of the input exergy was destroyed. Other main sources of exergy destruction rate are the solar heat pipe evaporator condenser, at 6.655 kW; then the turbine, at 6.228 kW; and the water preheater, at 0.907 kW. The overall energetic and exergetic efficiencies of the combined solar system was 69.57% and 12.41%, respectively.

Review History:

Received: 22 Aug. 2018

Revised: 11 Dec. 2018

Accepted: 11 Mar. 2019

Available Online: 3 May. 2019

Keywords:

Energy efficiency

Exergy efficiency

Solar heat pipe system

Regenerative organic Rankine cycle

1- Introduction

The demand and utilization of energy around the world have been constantly increased since the industrial revolution. In parallel to, the primary demands of energy in the world have been predicted to rise up by about 50% from 2016 to 2030 years [1]. By considering the environmental effects of fossil fuels, renewable energies are getting popular all over the world. Solar energy is an ideal source of energy because of its availability. Both the thermal and electrical energies can be produced from the sunlight. In the recent years, the use of solar systems is rising more and more all over the world. This technology can play an effective role in the industry by converting the solar energy into the electricity and heating, without greenhouse emissions [2]. A heat pipe is an evaporation–condensation device for transporting thermal energy in which the latent heat of vaporization is used to transport without an appreciable temperature drop. The heat transport is realized by means of evaporating a liquid in the heat inlet section and subsequently condensing the vapor in a heat rejection area. This minimizes heat loss from the transporting fluid, when incident radiation is low [3]. Kasaeian et al. [4] reviewed solar collectors and photovoltaics as combined heat and power systems. They showed that, there are limited studies on the economic and exergy assessments of the solar Combined Heating and Power (CHP) systems. Sharaf and Orhan [5] carried out comparative thermodynamic analysis of densely-packed concentrated photovoltaic

thermal solar collectors in thermally in series and in parallel receiver configurations. Their study results show that, from an environmental viewpoint, both configurations are found capable of displacing a considerable amount of primary energy and CO₂ emissions. Al Zahrani and Dincer [6] carried out thermodynamic analysis of an integrated transcritical carbon dioxide power cycle for concentrated solar power systems. They conducted that, the studied power cycle achieved energy and exergy efficiencies of 34% and 82%, respectively. Shafieian et al. [7] reviewed latest developments, progress, and applications of heat pipe solar collectors. They provided an overview of the recent studies on heat pipe solar collectors, their utilization in different applications, and future research potentials. Hui et al. [8] performed building integrated heat pipe photovoltaic-thermal system for use in Hong Kong. Their simulation results showed that the annual water heating efficiency and electricity generation efficiency were around 35% and 10% respectively. Chaudhry et al. [9] reviewed heat pipe systems for heat recovery and renewable energy applications. Their review established that standard tubular heat pipe systems present the largest operating temperature range in comparison to other systems and therefore offer viable potential for optimization and integration into renewable energy systems. Jouhara et al. [10] carried out heat pipe based systems advances and applications. They conducted that, the use of heat pipe technology in heat exchange and thermal management of challenging scenarios is expanding fast due to their advantageous characteristics compared with conventional heat exchangers and temperature control systems. Advances in the design and capabilities

*Corresponding author's email: vbeygzadeh@gmail.com



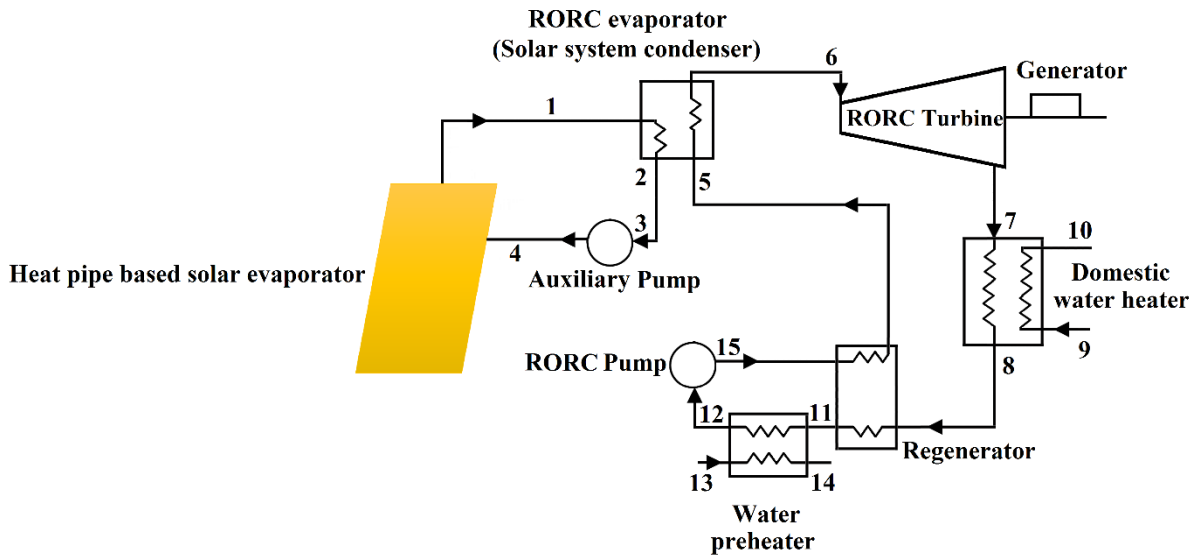


Fig. 1. Schematic of the proposed system.

of heat pipes have led to the development of cost-effective manufacturing techniques for both wicked and wickless heat pipes. Azad [11] studied three types of heat pipe solar collectors. He represented the comparative characteristics of the three collectors when operating under variable conditions. The first law of thermodynamics provides the concept of energy, which is defined based on empirical knowledge as a physical quantity of the state of thermodynamic systems. In reality energy presents itself in various forms such as thermal, mechanical, chemical, electrical, magnetic, photonic energy, etc. These various forms of energy can be converted into one another with some restriction in thermal energy. The first law also expresses the empirical principal that the total amount of energy is conserved whatever energy conversion may take place. The law of conservation of energy indicates that energy never disappears, while the second law of thermodynamics sets forth that thermal energy cannot be fully utilized so far as we are in our atmospheric environment. Engineering thermodynamics has recently introduced a new energy quantity called exergy to figure out how much work or power we can utilize from a given amount of energy with respect to the natural environment. Energy is conserved in any processes; whereas, exergy is dissipated in spontaneous processes. Exergy analyses are thus effective in improving the energy efficiency in practical manufacturing processes [12]. Iran is located on the solar belt and is among the countries which enjoy a high solar potential and is considered as one of the best places for utilization of this source of energy [13]. Due to the benefits of novel integrated solar based energy systems for Iran sustainable development, in this study, a novel Solar Combined Heating and Power (SCHP) system with a Solar Heat Pipe Evaporator (SHPE), a SHPE condenser, a turbine, a Water Pre-Heater (WPH), a Domestic Water Heater (DWH), a regenerator, a pump and an auxiliary pump is thermodynamically modelled and assessed with energy and exergy analyses. The main aims are to improve understanding of this SCHP system and suggestion a new efficient and inexpensive solar thermal system with long life

cycle. The following specific tasks are conducted:

To model and to simulate (with Engineering Equation Solver (EES) software) and validate the SCHP system.

To apply energy and exergy analyses of the SCHP system to determine the energy flow and exergy destruction rate of each component and energy and exergy efficiencies of the SCHP system.

To conduct a comprehensive parametric study to determine the effect of major design parameters on SCHP system performance.

The system description and assumptions are presented next. Then, system modeling, results and discussion, and conclusions are presented, respectively.

2- Material and Methods

In this section, the specifications of the SCHP system and its components are introduced.

2- 1- System description

Fig. 1 indicates a SCHP system composed of a SHPE (which is composed of 5410 heat pipes), an auxiliary pump, a SHPE condenser, a turbine, an electrical generator, a DWH, a regenerator, a WPH and a Regenerative Organic Rankine Cycle (RORC) pump.

This system uses the solar energy to vaporize a working fluid (toluene in this study) through the SHPE, which drives SHPE condenser (RORC evaporator) and vaporize RORC working fluid (Isohexane in this study).

To carry out the thermodynamic analysis of the SCHP system, this presumptions are used:

- All the processes are at steady state.
- Heat losses from piping and other components are zero.
- All of the Solar Heat Pipe System (SHPS) components are adiabatic except SHPE.
- Pressure drops in vapor and liquid headers, vapor and liquid lines, compensation chamber and RORC cycle were neglected.
- The dead state is $P_0 = 101 \text{ kPa}$ and $T_0 = 298.15 \text{ K}$.

Table 1. Input data for the SCHP system.

Turbine efficiency	85%	Working fluid	Isohexane
Pump efficiency	85%	SHPE condenser pinch point temperature, °C	2
DWH pinch point temperature, °C	2	WPH pinch point temperature, °C	2
Turbine inlet pressure, kPa	450	DWH type	Plate heat exchanger
Pump inlet pressure, kPa	29	SHPE condenser type	Plate heat exchanger
Turbine type	Single stage	WPH type	Plate heat exchanger

Table 2. Input data for the solar heat pipe system.

SHPE length, m	1.5	Liquid filling mass, kg	3.806
Overall heat loss coefficient from Heat pipes to ambient, kW/m ² .K	0.005	Heat pipes material	Black Nickel
SHPE heat removal factor	0.83	Critical radius of bubble generation for toluene, m	0.00000007
SHPE condenser operating pressure range, kPa	0-4500	SHPS condensers length, m	2
SHPE to SHPE condenser height difference, m	1	SHPE condenser height, m	2
Solar heat pipe system operating temperature range, °C	100-125	Heat pipes mesh ratio	1:1
Heat pipes layer	2	Heat pipes type	Mesh screen
Internal diameter of heat pipes vapor line, m	0.041	number of heat pipes	5410
Thickness of heat pipes wick, m	0.0075	Heat pipes porosity	0.64
Thickness of heat pipes secondary wick, m	0.005	Internal diameter of heat pipes, m	0.049
Thickness of heat pipes primary wick, m	0.0025	Effective diameter of wick pores, m	0.1111
External diameter of heat pipes evaporator, m	0.05	SHPS liquid and vapor lines material	Cast iron
SHPE condenser pressure drop, kPa	6	SHPS liquid line thickness, m	0.002
SHPE condenser conductivity, W/m.K	16	SHPS vapor line Length, m	3
Thermal conductivity of heat pipes evaporator, W/m.K	91	Heat pipes wall thickness, m	0.001
SHPS vapor line diameter, m	0.6	SHPS liquid line diameter, m	0.5
SHPE pressure drop, kPa	11	SHPS liquid line length, m	4
SHPS average stream speed, m/sec	50	SHPS vapor line thickness, m	0.002
Low content of Ferro oxide glass transmission factor, (τ)	0.91	Black nickel absorption factor (α)	0.96

- The ambient average temperature is $T_{amb} = 299.15$ K.
- The mean solar radiation during the SCHP operation period of 8:00 until 17:00 was 400 W/m².
- There is an axisymmetric stream in all the parts of the SHPS.
- Chemical exergy of components and the kinetic, potential energy and exergy are neglected.

3- Analysis

For thermodynamic modeling, the SCHP (Fig. 1), the equations developed are programmed using engineering equation solver software. It should be noted that, the gravity effect pressure which created by the height difference between the RORC evaporator and the SHPE is +14.936 (obtained using hydrostatic pressure equation) and considered in thermodynamic modeling of the SCHP system. Mass, energy and exergy balances for any control volume at steady state operation with negligible potential and kinetic energy changes can be expressed, respectively, by

$$\sum_k \dot{m}_i - \sum_k \dot{m}_e = \frac{dm_{cv}}{dt} \quad (1)$$

$$\frac{dE_{cv}}{dt} = \sum \dot{Q}_{cv} - \dot{W}_{cv} + \sum_i \dot{m}_i h_i - \sum_e \dot{m}_e h_e \quad (2)$$

$$\frac{d\psi_{cv}}{dt} = \sum_i \dot{m}_i \psi_i - \sum_e \dot{m}_e \psi_e + \sum_j \left(1 - \frac{T_0}{T_j}\right) \dot{Q}_j - (\dot{W}_{cv} - P_0 \frac{dV_{cv}}{dt}) - \dot{I}_{cv} \quad (3)$$

And the specific exergy is given by

Table 3. The operating limits of the SHPS.

Entrainment limit	Viscous limit	Sonic limit	Boiling limit	Filled liquid Mass limit
\dot{Q}_{EL} (kW)	\dot{Q}_{VL} (kW)	\dot{Q}_{SL} (kW)	\dot{Q}_{BL} (kW)	\dot{Q}_{FL} (kW)
2066	41332	248838	911704	597.367

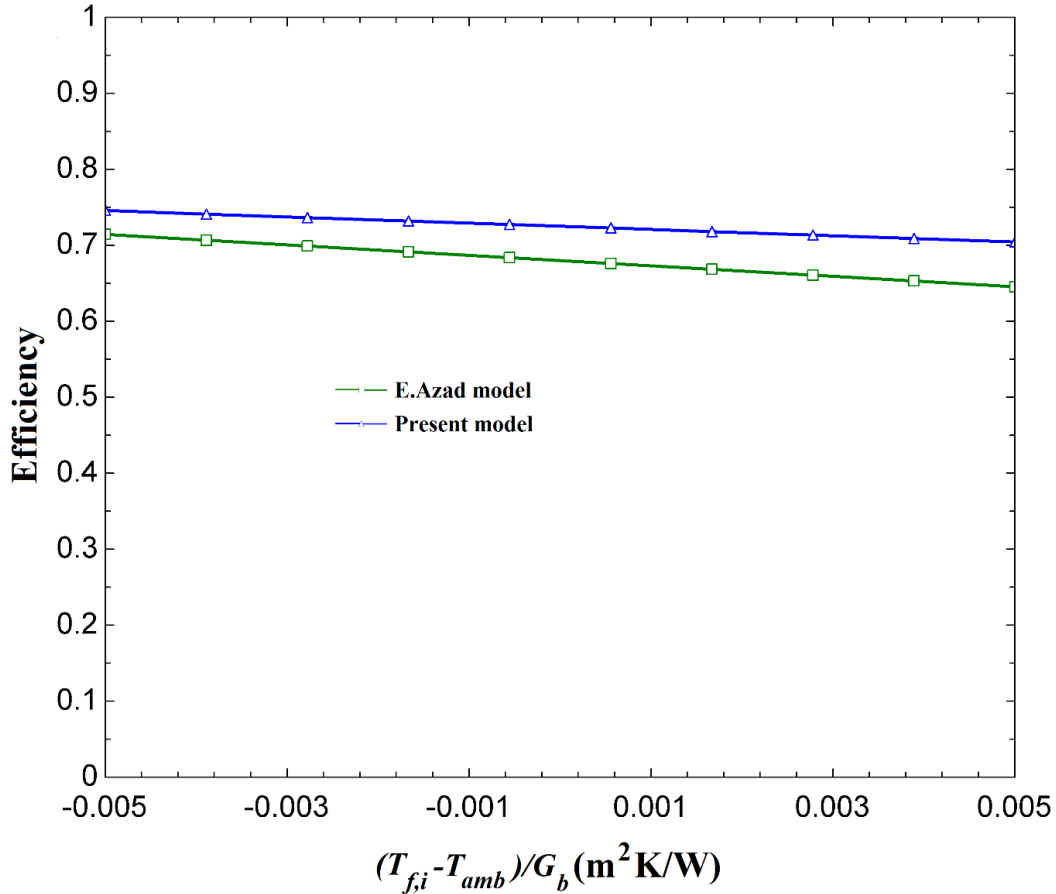


Fig. 2. Validation of the SHPE model as compared with Azad [11].

$$\psi = (h - h_0) - T_0(s - s_0) \tag{4}$$

Then the total exergy rate associated with a fluid stream becomes

$$\dot{E} = \dot{m}\psi \tag{5}$$

The input data for thermodynamic modeling of the SCHP system are given in Tables 1 and 2.

In the SHPS with auxiliary pump, the system heat transfer capacity will be controlled by five limits (boiling, entrainment, viscous, sonic and liquid filling mass limits). According to [14], the heat transfer limits of the SHPS is shown in Table 3.

The governing equations for the SCHP system are listed in Table 4. It should be noted that, for the thermodynamic

analysis of the SHPS, we considered the method used by Duffie and Beckman [15].

4- Results and Discussion

In this section, the results of thermodynamic modeling of the solar SCHP system are presented, containing assessments of the effects of varying three design parameters on SCHP system performance.

4- 1- Validation of the SHPE model

The SHPE model is validated against the experimental study by Azad [11], as shown in Table 5 (at point $(\frac{T_{f,i} - T_{amb}}{G_b} = 0)$) and Fig. 2. The model shows good agreement with the experimental work. The little deviation in the simulations as compared to the experimental results is due to the systems modeling conditions (for example, solar radiation intensity).

4- 2- Validation of the SCHP cycle model

The analysis of the SCHP cycle is validated with the U.S.

Table 4. The governing equations for the SCHP system.

The useful heat gained by the SHPS	$\dot{Q}_u = \dot{m}_1(h_1 - h_4)$
The useful power produced by the SHPS	$\dot{Q}_u = A_{SOL,EVA} F_R (S - U_l (T_4 - T_{amb}))$
The SHPE effective area	$A_{SOL,EVA} = 0.75 \times N_{HP} \pi D_o L_{HP}$
Heat removal factor	0.83
Radiation flux absorbed by the SHPE	$S = \eta_{HP} G_b$
Heat pipes optical efficiency	$\eta_{HP} = \tau \alpha$
The energy efficiency of the SHPE	$\eta_{en,SOL,EVA} = \frac{\dot{Q}_u}{G_b A_{SOL,EVA}}$
The inlet exergy of the SHPE	$\dot{E}_{SUN} = G_b A_{SOL,EVA} \left(1 + \frac{1}{3} \left(\frac{T_{amb}}{T_{SUN}}\right)^4 - \frac{4}{3} \left(\frac{T_{amb}}{T_{SUN}}\right)\right)$
The sun temperature	4500 K
The exergy destruction rate of the SHPE	$\dot{I}_{SOL,EVA} = \dot{E}_4 - \dot{E}_1 + \dot{E}_{SUN}$
The auxiliary pump work	$\dot{W}_{AP} = \dot{m}_3(h_4 - h_3)$
The auxiliary pump exergy balance	$\dot{I}_{AP} = \dot{E}_3 + \dot{W}_{AP} - \dot{E}_4$
The turbine energy balance	$\dot{W}_{OT} = \dot{m}_6(h_6 - h_7)$
The turbine exergy balance	$\dot{I}_{OT} = \dot{E}_6 - \dot{E}_7 - \dot{W}_{OT}$
The DWH energy balance	$\dot{m}_7(h_7 - h_8) = \dot{m}_{DWH}(h_{10} - h_9)$
The DWH exergy balance	$\dot{I}_{DWH} = \dot{E}_9 + \dot{E}_7 - \dot{E}_{10} - \dot{E}_8$
The regenerator energy balance	$\dot{m}_8(h_8 - h_{11}) = \dot{m}_5(h_5 - h_{15})$
The regenerator exergy balance	$\dot{I}_{REG} = \dot{E}_{15} + \dot{E}_8 - \dot{E}_{11} - \dot{E}_5$
The WPH energy balance	$\dot{m}_{11}(h_{11} - h_{12}) = \dot{m}_{WPH}(h_{14} - h_{13})$
The WPH exergy balance	$\dot{I}_{WPH} = \dot{E}_{13} + \dot{E}_{11} - \dot{E}_{12} - \dot{E}_{14}$
The pump work	$\dot{W}_{OP} = \dot{m}_{12}(h_{15} - h_{12})$
The pump exergy balance	$\dot{I}_{OP} = \dot{E}_{12} + \dot{W}_{OP} - \dot{E}_{15}$
The energy efficiency of the SCHP system	$\eta_{en} = \frac{\dot{Q}_{DWH} + \dot{Q}_{WPH} + \dot{W}_{OT}}{G_b A_{SOL,EVA}}$
The exergy efficiency of the SCHP system	$\eta_{ex} = \frac{\dot{W}_{OT} + \dot{E}_{WPH,o} - \dot{E}_{WPH,i} + \dot{E}_{DWH,o} - \dot{E}_{DWH,i}}{\dot{E}_{SUN}}$

Table 5. Validation of the SHPE model.

Azad [11] study	Present study
Heat pipe solar collectors efficiency: Type 1: 60% Type 2: 66% Type 3: 68%	Heat pipe solar collector efficiency: 72.51%

Table 6. Validation of the SCHP system model.

U.S. Department of Energy data	Present study
Overall CHP cycle efficiency: 65-75%	Overall SCHP cycle efficiency: 69.57%

Table 7. The thermodynamic properties of points for the SCHP system at indicated nodes in Fig. 1.

State	Fluid	\dot{m} (kg/s)	T (°C)	P (kPa)	h (kJ/kg)	s (kJ/kg.K)	\dot{E} (kW)
1	Toluene	0.5	125	150.7	380.5	0.9566	57.47
2	Toluene	0.5	28.84	144.7	-151.6	-0.4429	0.04627
3	Toluene	0.5	28.84	159.6	-151.5	-0.4429	0.05493
4	Toluene	0.5	28.84	161.7	-151.5	-0.4429	0.05614
5	Isohexane	0.52	26.84	450	-77.34	-0.246	0.2863
6	Isohexane	0.52	122.6	450	434.3	1.143	51.06
7	Isohexane	0.52	75.54	29	355.8	1.183	3.992
8	Isohexane	0.52	27	29	268.7	0.9144	0.3415
9	Water	0.2229	25	200	104.9	0.3669	0.02213
10	Water	0.2229	73.54	200	308	0.9978	3.349
11	Isohexane	0.52	25.65	29	266.5	0.9068	0.3363
12	Isohexane	0.52	25.65	29	-80.36	-0.254	-0.05689
13	Water	43.12	23.65	200	99.3	0.348	4.832
14	Water	43.12	24.65	200	103.5	0.362	4.318
15	Isohexane	0.52	25.83	450	-79.6	-0.2536	0.2811

Department of Energy’s Office of Energy Efficiency and Renewable Energy data, as shown in Table 6. The results show a very good agreement between the current SCHP system model and the U.S. Department of Energy data.

4- 3- Energy and exergy analysis results

The thermodynamic properties of states for the SCHP system at indicated nodes in Fig. 1 are summarized in Table 7. The energy analysis results are summarized in Table 8.

Table 8. The results of energy analysis of the SCHP system.

SHPE useful energy	266 kW
DWH energy flow	45.25 kW
WPH energy flow	180.4 kW
SHPE condenser energy flow	266 kW
RORC turbine net power	40.44 kW
RORC pump input power	0.3974 kW
Auxiliary pump input power	0.001414 kW
Combined cycle efficiency	69.57%

Table 9. The results of exergy analysis of the SCHP system.

SHPE exergy destruction rate	291.1 kW
DWH exergy destruction rate	0.3234 kW
SHPE condenser exergy destruction rate	6.655 kW
RORC turbine exergy destruction rate	6.228 kW
RORC pump exergy destruction rate	0.05945 kW
WPH exergy destruction rate	0.907 kW
Auxiliary pump exergy destruction rate	0.0002093 kW
Combined cycle efficiency	12.41 %

The exergy analysis results are summarized in Table 9, and show that the highest exergy destruction rate happens in the SHPE, which is 291.1 kW.

4- 4- Effect of varying SHPE condenser pinch point temperature on combined cycle performance

Fig. 3 shows the variation with SHPE condenser pinch point temperature of the energy efficiency and exergy efficiency. As shown in this figure, increasing SHPE condenser pinch point temperature reduces the heat absorbed by the SHPE condenser, hence the enthalpy of the Isohexane vapor in the SHPE condenser decreases, which increases the SCHP exergy destruction rate and leads to a decrease in the energy and exergy efficiencies of the SCHP.

4- 5- Effect of varying solar radiation intensity on combined cycle performance

Fig.4 shows the variation of energy efficiency and exergy efficiency with solar radiation intensity. As can be seen, increasing solar radiation intensity, increases the energy and exergy efficiencies of the SCHP system, due to an increase in

the solar radiation intensity, decreases the SHPE heat losses and exergy destruction rate.

4- 6- Effect of varying SHPE heat removal factor on combined cycle performance

Fig.5 shows the variation of energy efficiency and exergy efficiency with SHPE heat removal factor. When the SHPE heat removal factor increases, the SCHP system total irreversibility decreases, hence improves the SCHP system performance.

5- Conclusions

In this study, the steady state thermodynamic analysis of the SCHP system is conducted under Tabriz, Iran, summer and spring conditions. This study intends to introduce a novel localized and efficient system for combined production of heating and power. The results of thermodynamic analysis showed that the main source of the exergy destruction is the SHPE. In the SHPE, 291.1 kW of the input exergy was destroyed. Other main sources of exergy destruction are the SHPE condenser, at 6.655 kW; then the RORC turbine, at

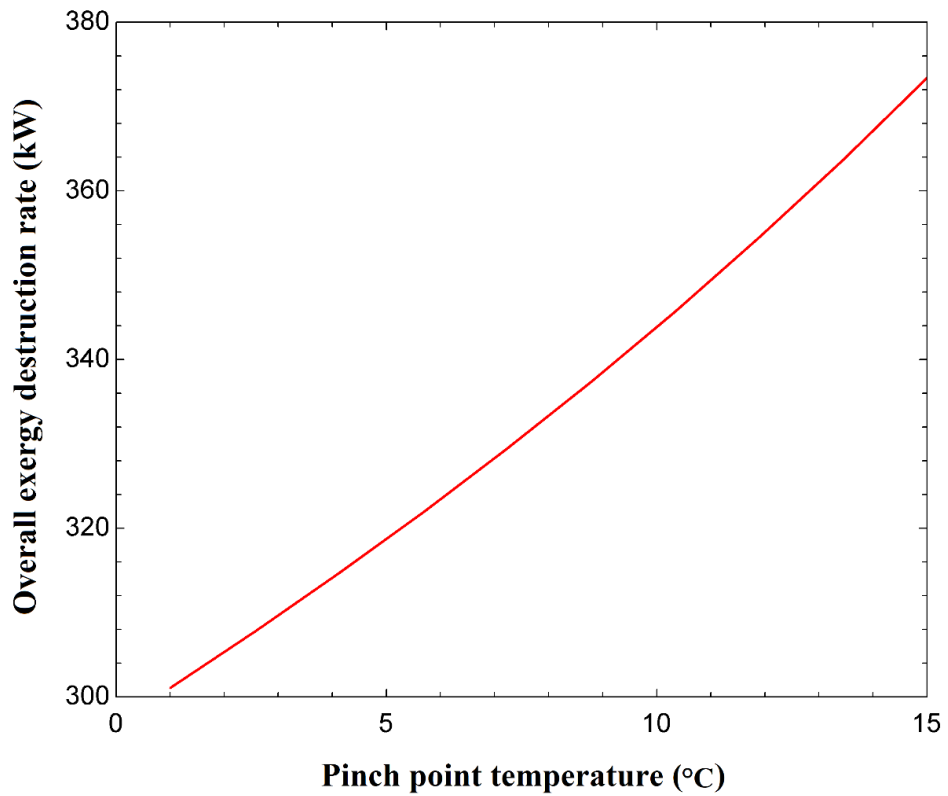
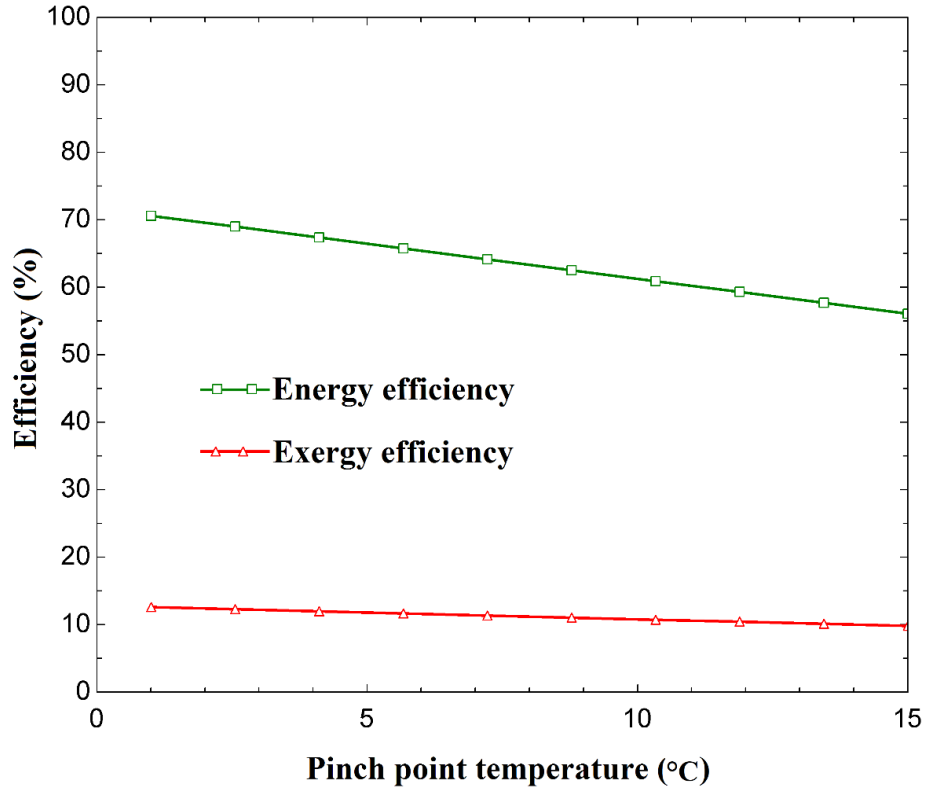


Fig. 3. Variation with SHPE condenser pinch point temperature of the energy efficiency and exergy efficiency.

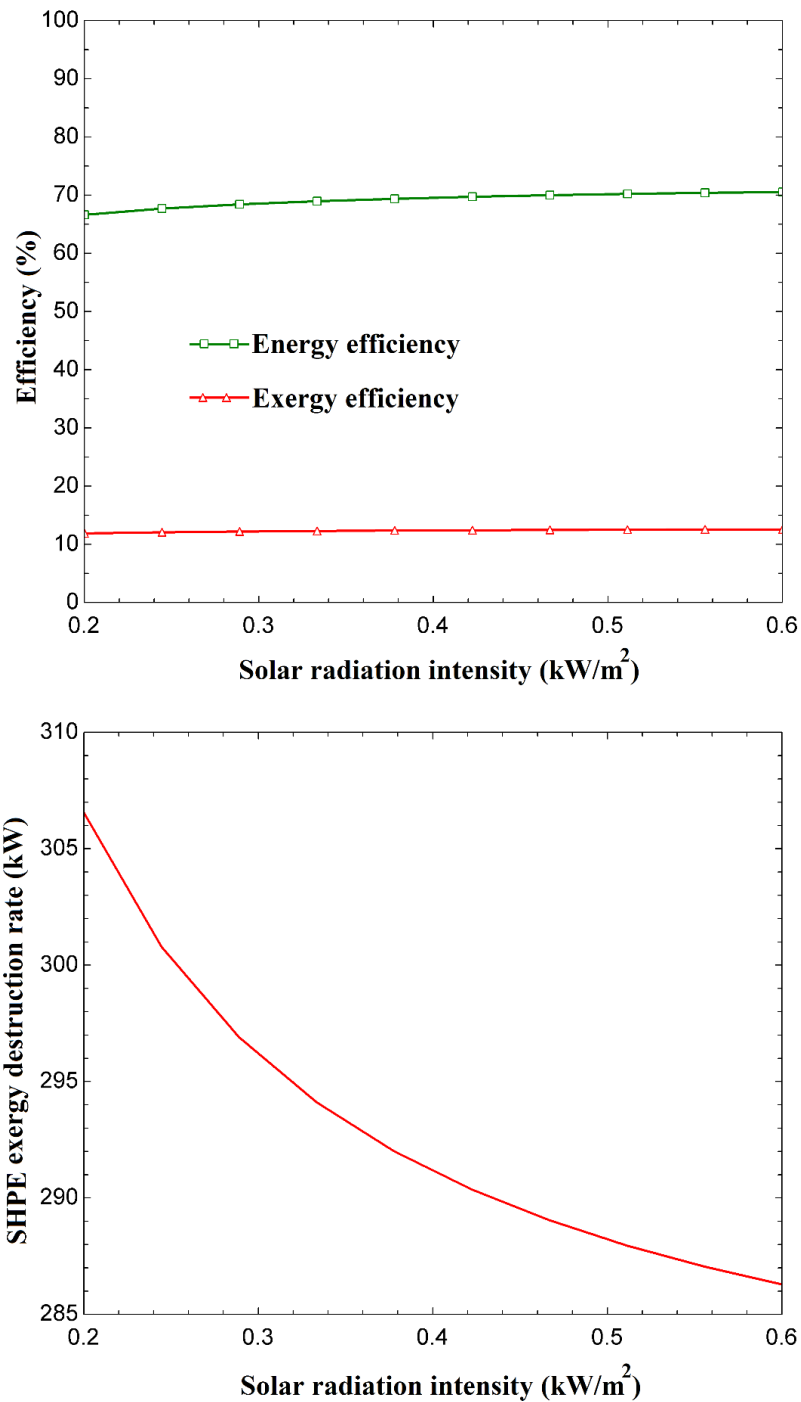


Fig. 4. Variation with solar radiation intensity of the energy efficiency and exergy efficiency.

6.228 kW; and the WPH, at 0.907 kW. The overall energetic and exergetic efficiencies of the SCHP was approximately 69.57% and 12.41%, respectively. Other main conclusions follow:

- Increasing SHPE condenser pinch point temperature, leads to a decrease in the energy and exergy efficiencies of the SCHP.
- Increasing solar radiation intensity, increases the energy

and exergy efficiencies of the SCHP system.

- Increasing SHPE heat removal factor, increases the energy and exergy efficiencies of the SCHP system.

Acknowledgements

The author is thankful to the management and staff of NIORDC for their technical support.

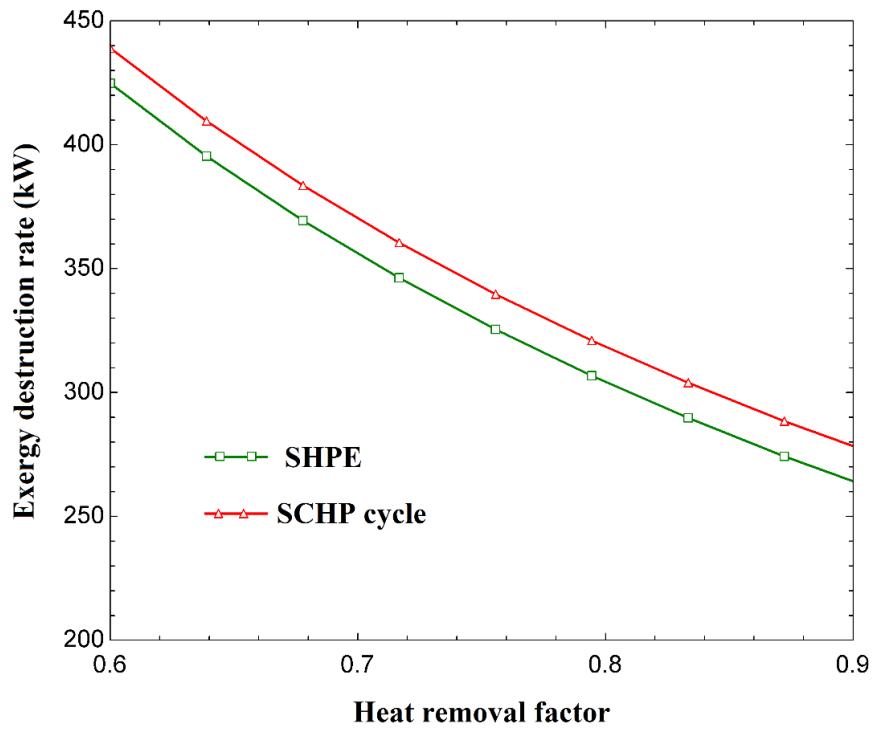
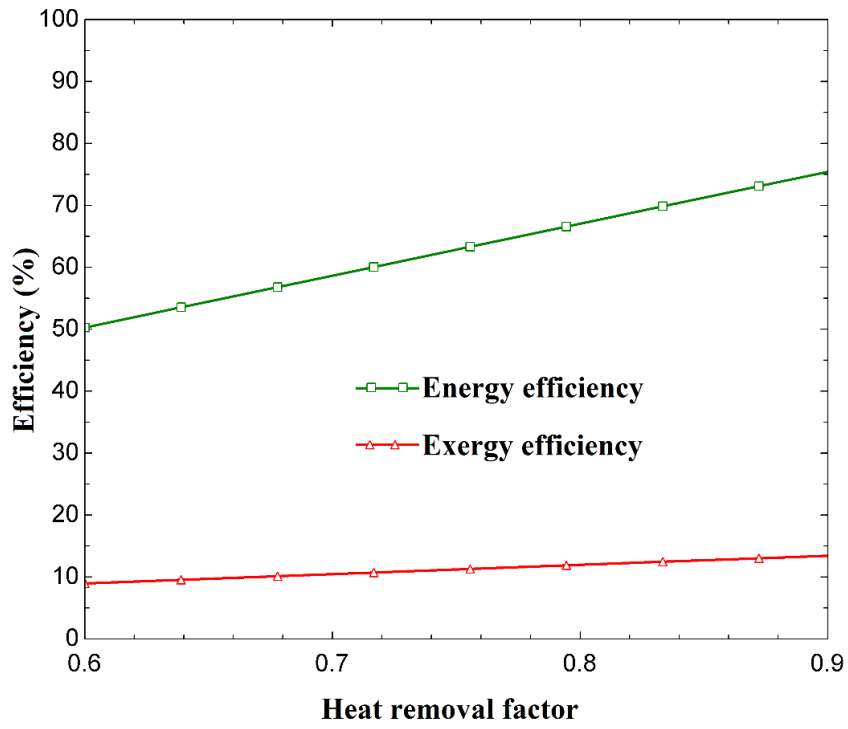


Fig. 5. Variation with SHPE heat removal factor of the energy efficiency and exergy efficiency.

Nomenclature	
A	Area, m ²
D	Diameter, m
\dot{E}	Exergy rate, kW
E	Energy, kW
G_b	Solar radiation, kW/m ²
F_R	Solar heat pipe evaporator heat removal factor
h	Specific enthalpy, kJ/kg
i	Exergy destruction rate, kW
L	Length, m
\dot{m}	Mass flow rate, kg/s
m_f	Solar heat pipe evaporator liquid filling mass, kg
m	Mass, kg
N	Number
P	Pressure, kPa
\dot{Q}	Heat rate, kW
S	Radiation absorbed by the solar heat pipe evaporator
s	Specific entropy, kJ/kg.K
T	Temperature, K
t	Time, s
U_l	Overall heat loss coefficient from heat pipes to ambient, kW/m ² .K
V	Volume, m ³
\dot{W}	Work rate, kW
Greek symbols	
η	Efficiency
ψ	Specific exergy, kJ/kg
η_{HP}	Heat pipe optical efficiency
δ	Thickness, m

τ	Transmission factor
α	Absorption factor
Subscripts	
AP	Auxiliary pump
amb	Ambient
cv	Control volume
DWH	Domestic water heater
BL	Boiling limit
EL	Entrainment limit
en	Energy
ex	Exergy
e	Exit
FL	Filled liquid Mass limit
f, i	Fluid entering solar heat pipe evaporator
HP	Heat pipe
i	Inlet
J _j	Component <i>j</i>
k	Component <i>k</i>
OP	RORC pump
OT	RORC turbine
o	Out
REG	Regenerator
SL	Sonic limit
SUN	Sun
SOL, EVA	Solar heat pipe evaporator
u	Useful
VL	Viscous limit
WPH	Water preheater
0	Dead state

References

- [1] F.Yilmaz, M.Ozturk, R.Selbas, Energy and exergy performance assessment of a novel solar-based integrated system with hydrogen production, *Int.J.Hydrogen Energ.*, 44(34) (2019) 18732– 18743.
- [2] A.Moaleman, A.Kasaeian, M.Aramesh, O.Mahian, L.Sahota, G.N.Tiwari, Simulation of the performance of a solar concentrating photovoltaic-thermal collector applied in a combined cooling heating and power generation system, *Energy Convers. Manag.*, 160(1) (2018) 191–208.
- [3] E. Azad, Theoretical analysis to investigate thermal performance of co-axial heat pipe solar collector, *Heat and Mass Transfer*, 47(1) (2011) 1651–1658.
- [4] A.Kasaeian, G.Nouri, P.Ranjbaran, D.Wen, Solar collectors and photovoltaics as combined heat and power systems: A critical review, *Energy Convers. Manag.*, 156(1) (2018) 688–705.
- [5] O.Z. Sharaf, M.F Orhan, Comparative thermodynamic analysis of densely-packed concentrated photovoltaic thermal (CPVT) solar collectors in thermally in-series and in-parallel receiver configurations, *Renew. Energ.*, 126(1) (2018) 296-321.
- [6] A.A. Alzahrani, I.Dincer, Thermodynamic analysis of an integrated transcritical carbon dioxide power cycle for concentrated solar power systems, *Sol. Energy*, 170(1) (2018) 557–567.
- [7] A.Shafieian, M.Khiadani, A.Nosrati, A review of latest developments, progress, and applications of heat pipe solar collectors, *Renew. Sust. Energ. Rev.*, 95(1) (2018) 273-304.
- [8] L.Hui, C.T.Tai, J.Jie, Building-integrated heat pipe photovoltaic/thermal system for use in Hong Kong, *Sol. Energy*, 155(1) (2017) 1084-1091.
- [9] H.N.Chaudhry, B.R.Hughes, S.A.Ghani, A review of heat pipe systems for heat recovery and renewable energy applications. *Renew. Sust. Energ. Rev.*, 16(1) (2012) 2249– 2259.
- [10] H. Jouhara, A. Chauhan, T. Nannou, S. Almahmoud, B. Delpech, L.C. Wrobel, Heat pipe based systems-Advances and applications, *Energy*, 128(1) (2017) 729-754.
- [11] E. Azad, Assessment of three types of heat pipe solar collectors, *Renew. Sust. Energ. Rev.*, 16(5) (2012) 2833– 2838.
- [12] N.Sato, *Chemical Energy and Exergy*, Elsevier Science, 2004.
- [13] Iran Renewable Energy and Energy Efficiency Organization Annual report, 2010-2017.
- [14] Chi SW, *Heat Pipe Theory and Practice: A Source Book*, Hemisphere Pub. Corp, 1976.
- [15] J.A. Duffie, W.A. Beckman. *Solar Engineering of Thermal Processes*, John Wiley & Sons, Inc., 2013.

